2024 IEEE/RSJ International Conference on Intelligent Robots and Systems (IROS)
October 14-18, 2024. Abu Dhabi, UAE

Time-varying Control Barrier Function for Safe and Precise Landing of a UAV on a Moving Target

Viswa Narayanan Sankaranarayanan*, Akshit Saradagi, Sumeet Satpute, and George Nikolakopoulos

***Abstract*— In this article, we present a control barrier function (CBF)-based control strategy for safe and precise landing of an unmanned aerial vehicle (UAV) on a moving target. The CBF is time-varying, as it depends on the velocity of the landing platform and captures three crucial safety constraints: (a) collision avoidance with the landing platform, (b) precise vertical descent on a narrow landing platform, and (c) ground clearance throughout the landing maneuver. The proposed CBF's parameters can be adjusted to set the desired width and height of the descending cone. A quadratic program-based CBF safety filter is designed, which takes a nominal position tracking control input and yields a minimally invasive control input that enforces the safety constraints throughout the landing maneuver. The controller's feasibility is analyzed and its performance is validated through multiple experiments using a quadrotor UAV and an unmanned ground vehicle.**

I. Introduction

The applications involving the coordination of unmanned aerial vehicles (UAVs) and unmanned ground vehicles (UGVs) have expanded significantly in recent years. A crucial challenge in the coordination of ground and aerial robots is to land the aerial robot on the moving UGV [1]. While the landing problem has been widely investigated from the perspectives of the mechanical design of the landing gear, detection of the landing platform, and pre-planned trajectory tracking [2], a systematic control design approach that guarantees precision and safety throughout the landing maneuver has not yet been well investigated.

In the landing scenario, the UAV is prone to collision with the target robot and undesirable ground effects. A generic engineering solution to this problem involves a multi-stage switching approach, where the UAV ascends to a safe altitude, approaches the platform horizontally to align over the platform, and descends to the platform's surface while maintaining the alignment. The control schemes using vision-based guidance [3], [4] assume that the UAV is initialized at a convenient altitude to enable tracking of the target, and therefore, the focus is on the approach phase through visual servoing. On the other hand, the conventional robust [5] and adaptive [6] controllers, proposed in the literature for UAV landing, address either the approach or the descending phase, assuming the availability of reliable solutions for the other phases of the landing maneuver.

*Corresponding author

The authors are with the Robotics and Artificial Intelligence Group of the Department of Computer Science, Electrical and Space Engineering at Luleå University of Technology, Sweden. This work has been partially funded by the European Union's Horizon 2020 Research and Innovation Programme AERO-TRAIN under the Grant Agreement No. 953454.

Another crucial aspect of the UAV landing scenario is the stringent requirements on precision, especially when the area available for landing is small, as the UAV is expected to deliberately perform a precise contact maneuver with the landing platform. Vision-guided control schemes have addressed this aspect as a precise alignment problem with the fiducial markers placed on the landing platform [7], [8]. In contrast, the robust control techniques [9] address this problem through prescribed performance control. The landing trajectory design with avoidance is handled using an external planner in these methods. In this article, we propose a control barrier function-based approach that does not rely on pre-planned trajectories but accommodates the safety and precision constraints directly into the control design and shapes the UAV's trajectory on the fly.

The safety constraints can be enforced in control very elegantly using a control barrier function (CBF) technique [10]. In this approach, a safe set, defined as the super level set of a control barrier function is rendered forward invariant and asymptotically stable throughout a control execution. The CBF filter, in the form of a quadratic program [10], is used to enforce the safety constraints over a nominal controller. Recently, CBFs have been used with UAVs mainly for collision avoidance [11] and visual surveillance [12]. Although methods such as [13], [14] use a CBF approach for a landing problem, the CBF is constructed only to bound the error in trajectory tracking, similar to prescribed performance control, rather than enforcing the constraints directly for a smooth and safe landing. However, in our case, the CBF must provide avoidance in some regions, while still allowing to establish contact with the target vertically.

Contributions: The contributions of this work are as follows. (a) A novel time-varying CBF (TV-CBF) is designed based on methodical analysis of three crucial safety constraints (Figure 1) for safe and precise landing: a no-go zone around the ground robot, smooth final vertical descent, and prescribed ground clearance in the vicinity of the ground robot. The design parameters provide the flexibility to shape the unsafe region for the desired vertical descent. (b) This proposed CBF approach leads to smooth landing maneuvers from a large set of initial conditions, as against switched and multi-stage maneuvers found in literature, which are initiated from special initial conditions. (c) A control scheme is proposed, where the CBF filter is presented in the form of a simple quadratic program that works with a nominal position tracking controller to track and land on the moving target. (d) The controller's performance is tested with experiments using static and moving targets.

979-8-3503-7769-9/24/$31.00 ©2024 IEEE

II. Notations and Preliminaries

We denote by $\mathbb{R}$ the set of real numbers, by $\mathbb{S}$ the unit circle, and by $\mathbf{I}_n$ an identity matrix of size n. The boundary of a time-varying set $S(t)$ is denoted as $\partial S(t)$. A continuous function $\alpha : (-b, a) \to (-\infty, \infty)$, where the real constants $a, b > 0$, is said to be an extended class-$\mathcal{K}$ function if $\alpha(0) = 0$ and it is strictly increasing. Next, we present some important ideas and results from the theory of control barrier functions, which is the design methodology employed in this work to ensure safety during the landing maneuver.

Let $S(t) \subset \mathcal{X}$ be the region of the state-space, which is deemed as a time-varying safe region for the operation of a control affine dynamical system $\dot{x} = f(x) + g(x)u$. Let $h(x,t) : D(t) \subset \mathcal{X} \to \mathbb{R}$ be a continuously differentiable function, with $S(t) \subset D(t)\ \forall t$, such that $S(t) := \{x \in \mathcal{X} \mid h(x,t) \geq 0\}$, that is, $S(t)$ is a zero super-level set of the function $h(x,t)\ \forall t$. The time-varying set $S(t)$ is rendered safe, if the control input u ensures positive invariance of the set $S(t)\ \forall t$, that is, $x(t_0) \in S(t_0)$ implies $x(t) \in S(t)$ for all $t \geq t_0$. In addition, if $S(t)$ is rendered asymptotically stable when the system is initialized in $D(t) \setminus S(t)$, a measure of robustness can be incorporated into the notion of safety. The definition presented next provides conditions for a function $h(x,t)$ to be a valid time-varying control barrier function.

Definition 1 (Time-varying CBF [15]): A candidate continuously differentiable function $h(x,t)$ is a valid control barrier function for a control affine dynamical system $\dot{x} = f(x) + g(x)u$, if there exists a locally Lipschitz continuous class-$\mathcal{K}$ function ω such that, for all $(x,t) \in D(t) \times [0, \infty]$

$$\sup_{u \in \mathcal{U}} \frac{\partial h(x,t)}{\partial x}^{\mathrm{T}} (f(x) + g(x)u) + \frac{\partial h(x,t)}{\partial t} \geq -\omega(h(x,t)). \quad (1)$$

The forward invariance of $S(t)$ ($\dot{h}(x,t) \geq 0$ on $\partial S(t)$) and asymptotic stability of $S(t)$ ($\dot{h}(x,t) > 0$ in $D(t) \setminus S(t)$) are captured in one shot in the condition (1). In section IV-B, we present a time-varying control barrier function for the landing problem formulated in section III.

Proposition 1 ([10]): Let $\mathscr{S} \subset \mathscr{D}$ be the zero super-level set of a continuously differentiable function $h : \mathscr{D} \subset \mathcal{X} \to \mathbb{R}$. If h is a control barrier function on $\mathscr{D}$ and $\frac{\partial h(x)}{\partial x} \neq 0$ on $\partial \mathscr{C}$, then any Lipschitz continuous controller $u(x) \in K_h(x)$, where

$$K_h(x) = \{u \in \mathcal{U} \mid L_f h(x) + L_g h(x) u + \gamma \alpha(h(x)) \geq 0\} \quad (2)$$

for a control affine dynamical system renders $\mathscr{S}$ forward invariant and asymptotically stable in $\mathscr{D}$.

III. Problem Formulation

This section presents the modeling of UAV dynamics, a systematic analysis of the UAV landing scenario and the derivation of the control barrier function that encapsulates the safety constraints of the landing scenario.

A. Dynamics of quadrotor UAV

The UAV dynamics is given by,

$$m\ddot{\mathbf{p}}(t) + m\mathbf{G} = \tau_{\mathbf{p}}, \quad (3)$$

$$\mathbf{J}\ddot{\mathbf{q}}(t) + \mathbf{C}(\mathbf{q}, \dot{\mathbf{q}}, \mathbf{t})\dot{\mathbf{q}}(t) = \tau_{\mathbf{q}}, \quad (4)$$

.where $m, \mathbf{J} \in \mathbb{R}^3, \mathbf{C} \in \mathbb{R}^3$ are the mass, inertia and Coriolis terms of the UAV, $\mathbf{p}(t) \triangleq [x(t), y(t), z(t)]^{\mathrm{T}} \in \mathbb{R}^3$ is the position vector of the UAV defined in the inertial frame $\mathbf{X_W} - \mathbf{Y_W} - \mathbf{Z_W}$ (cf. Fig. 1), $\mathbf{G} \triangleq [0, 0, g]^{\mathrm{T}} \in \mathbb{R}^3$ is the gravity term, $\tau_{\mathbf{p}} \triangleq [\tau_x, \tau_y, \tau_z]^{\mathrm{T}} \in \mathbb{R}^3$ is the control input in the inertial frame, $\mathbf{q} \triangleq [\phi(t), \vartheta(t), \psi(t)]^{\mathrm{T}} \in \mathbb{S}^3$ is the orientation of the UAV, and $\tau_{\mathbf{q}} \in \mathbb{R}^3$ is the attitude control input.

B. Constraints for safe landing onto a moving platform

When the target position is available, a typical landing maneuver consists of three main stages: 1) Adjusting the altitude of the UAV to stay conveniently above the target platform, 2) Propelling horizontally to vertically align the UAV over the moving target platform, and 3) Initiating the descent onto the moving platform to complete the landing.

The proposed approach combines the three sequential steps into a single smooth and safe landing maneuver. We begin by deriving a set of three constraints that capture crucial concerns for safety in the landing maneuver. An

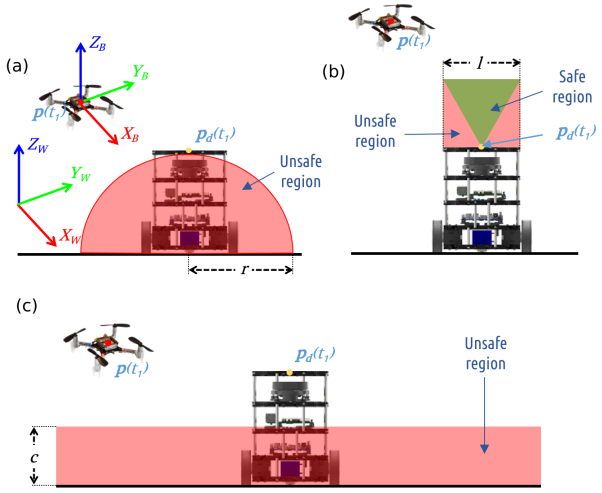

Fig. 1: Cross-sectional view of the landing constraints at time instant, $t = t_1$: (a) The UAV must avoid the hemispherical region (red) enclosing the robot; (b) In the landing proximity, the UAV must stay within a conical region (green) for vertical descent; (c) The UAV must maintain ground clearance.

essential problem in landing is collision avoidance with the ground robot (landing platform), which is modeled using a hemispherical unsafe region of radius r around the platform. The hemispherical constraint (cf. red region in Fig. 1a), centered at the platform's base, allows the UAV to avoid most parts of the landing platform while still being able to approach the platform from the top.

Secondly, to ensure smooth and precise vertical descent onto the landing spot, the safe region is marked as the descending cone (green triangle) in Fig 1b. The area outside the cone and above the target (red) is deemed unsafe. Furthermore, to reinforce safe operation and avoid turbulence effects arising from flying too close to the ground, the UAV must maintain a clearance, c from the ground (or from the water surface in case of a floating landing platform).

Such a constraint is imposed as a subspace constraint, as shown in Fig. 1c. Fig 2 illustrates a function (a candidate

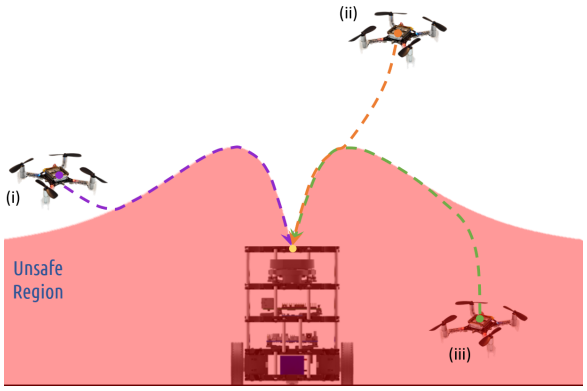

Fig. 2: Cross-sectional view of the proposed CBF with the unsafe zone (red) and the paths that a UAV is expected to follow from (i) a similar altitude as the landing platform, (ii) a higher altitude and (iii) inside the unsafe region.

control barrier function (CBF)) that captures the three safety constraints in the landing problem in one go. The expectations from the UAV landing maneuvers from three initial conditions are also illustrated. The UAV must complete the landing by staying in the white region and avoiding the red region, which is centered at the desired landing spot $\mathbf{p_d}(t) \triangleq [x_d(t), y_d(t), z_d(t)]^{\mathrm{T}}$ and moves with the target. Hence, the CBF constraint is time-varying in nature.

The safe zone is captured through the inequality:

$$e_z(t) >= \beta\alpha d(t)\exp(-\alpha d(t)), \tag{5}$$

where the horizontal distance $d(t) = \sqrt{e_x^2(t) + e_y^2(t)}$ is dependent on $\mathbf{p_d}(t) \triangleq [x_d(t), y_d(t), z_d(t)]^{\mathrm{T}}$, α, β are positive real scalars for stretching the CBF horizontally (cf. Fig. 3 (a)) and vertically (cf. Fig. 3 (b)), respectively, and $e_x(t), e_y(t), e_z(t)$ form the position error vector,

$$\mathbf{e_p}(t) = \begin{bmatrix} e_x(t) \\ e_y(t) \\ e_z(t) \end{bmatrix} = \begin{bmatrix} x(t) - x_d(t) \\ y(t) - y_d(t) \\ z(t) - z_d(t) \end{bmatrix}. \tag{6}$$

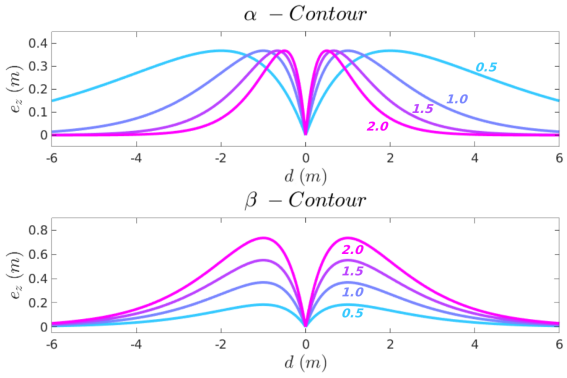

Fig. 3: CBF boundary contours for various: (a) α and (b) β

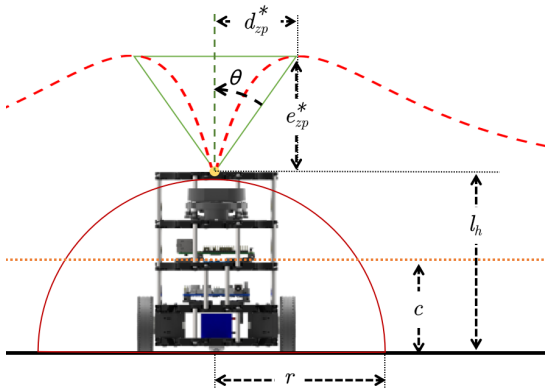

Fig. 4: Illustration of parameters needed for control design.

The descending cone's angle of inclination θ, and height e^*_{zp} (cf. Fig 4), i.e, the peak altitude of the CBF and the horizontal distance from the landing spot (d^*_{zp}) to the CBF's peak determine the parameters α & β. Their relationship is obtained by equating the gradient of the CBF with respect to the horizontal distance d to zero.

$$\frac{\partial h}{\partial d} = \alpha\beta(1 - \alpha d(t))\exp(-\alpha d(t)),$$
$$\frac{\partial h}{\partial d} = 0 \implies \alpha = \frac{1}{d^*_{zp}} = e^*_{zp}\tan(\theta). \tag{7}$$

From (7) and (5) we get, $\beta = e^*_{zp}\exp(1) = 2.718e^*_{zp}$. Further, we define the assumptions to formulate the control problem.

Assumption 1 (Initial error): The initial error values are bounded, such that $|e_x(0)|, |e_y(0)|, |e_z(0)| < b_1$. This assumption is necessary for any tracking controller.

Assumption 2 (Target velocity): The velocity of the ground robot is sufficiently smooth and bounded such that $|\dot{x}_d(t)| < v^x_m$, $|\dot{y}_d(t)| < v^y_m$, $\dot{z}_d(t) = 0$ implying that the landing spot's altitude remains constant.

Assumption 3 (Experimental procedure): Since this work focuses on modeling the safety constraints and control design, the experiments are carried out in a laboratory environment with the knowledge of UAV and target odometry, and no external disturbances.

With this premise, the formulation of the control design problem is presented next. **Problem Statement:** The problem considered in this article is that of designing a controller for landing a UAV defined by the dynamics (3)-(4) on a moving target, while enforcing the constraint (5) parameterized by the positive scalars α and β, under the assumptions 1 - 3.

IV. Proposed Control Solution

A. Control architecture for the UAV

The overall controller for the UAV is designed to have two loops [16] as shown in Fig 5. The position controller produces a pseudo-virtual input $\mathbf{u}'(t) = -\mathbf{K_p}\mathbf{e_p}(t) + \dot{\mathbf{p}}_\mathbf{d}$ to track the landing position ($\mathbf{p_d}$), where $\mathbf{K_p} \in \mathbb{R}^{3\times3}$ is a positive definite gain matrix. The CBF filter (described later

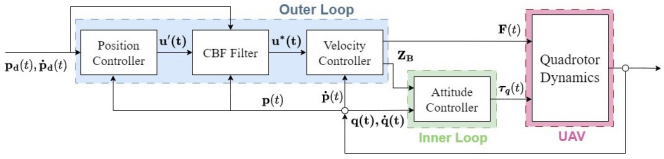

Fig. 5: A block diagram of the proposed control architecture.

in Subsection IV-C) then filters the pseudo-virtual input using the landing constraints and produces the actual virtual velocity input, $\mathbf{u}^*(t)$. The velocity controller produces the desired thrust using the virtual velocity input.

$$\tau_{\mathbf{p}}(t) = -\mathbf{K_v}(\dot{\mathbf{p}}(t) - \mathbf{u}^*(t)) + m\mathbf{G} \tag{8}$$

where $\mathbf{K_v} \in \mathbb{R}^{3\times3}$ is a positive definite gain matrix. The mapping of the thrust vector and further the attitude control input to the UAV's rotor velocities are achieved by standard geometric control method as in [17], [18], [19].

B. CBF constraints

The CBF filter is based on the position kinematic model of the UAV, $\dot{\mathbf{p}} = \mathbf{u}(t)$. The CBF filter acts in between the position and velocity controllers and it is assumed that the lower-level control layers track the velocity inputs in high speed and accuracy.

From the constraint in (5), we derive the following exponentially decaying barrier function which defines the safe set's boundary:

$$h(x,y,z,t) = e_z(t) - \beta\alpha d(t)\exp(-\alpha d(t)). \tag{9}$$

From (9), the gradients of the CBF involved in condition (1) are

$$\begin{aligned}
\frac{\partial h}{\partial x} &= -\frac{\alpha\beta e_x \exp(-\alpha d)(1-\alpha d)}{d} \\
\frac{\partial h}{\partial y} &= -\frac{\alpha\beta e_y \exp(-\alpha d)(1-\alpha d)}{d} \\
\frac{\partial h}{\partial z} &= 1 \\
\frac{\partial h}{\partial t} &= -\dot{z}_d + \frac{\alpha\beta(1-\alpha d)\exp(-\alpha d)(\dot{x}_d e_x + \dot{y}_d e_y)}{d}
\end{aligned} \tag{10}$$

where $\dot{z}_d = 0$. It is to be remarked that since $\dot{x}_d \& \dot{y}_d$ are external to the control inputs, $h(t)$ becomes time-varying. The forward invariance and asymptotic stability of the safe set $\mathscr{S} = \{x \in \mathbb{R}^3 \mid h(x) \geq 0\}$ is enforced by the CBF safety filter presented next.

C. CBF safety filter

For a valid time-varying control barrier function, condition (1) is satisfied for all $\mathbf{p} \in D(t)$ and $t \geq 0$. This implies that for all initial conditions in $D(t)$, there exists at least one control input from the admissible set $\mathscr{U} = [-v_m^x, v_m^x] \times [-v_m^y, v_m^y] \times [-v_m^z, v_m^z]$ that renders the safe set $S(t)$ forward invariant and asymptotically convergent, where $v_m^x, v_m^y, v_m^z \in \mathscr{R}^+$. It is remarked that for the safe operation of the UAV, these upper bounds are imposed on the velocity input for the UAV. We now present a CBF filter that takes the nominal control input $\mathbf{u}'(t)$ and yields the closest possible control input $\mathbf{u}^*(\mathbf{p},t)$ that guarantees safety.

$$\begin{aligned}
\mathbf{u}^*(\mathbf{p},t) &= \arg\min_{\mathbf{u}\in\mathscr{U}} ||\mathbf{u} - \mathbf{u}'(\mathbf{p},t)||^2 \\
\text{s. t. :} \ & \frac{\partial h(\mathbf{p},t)}{\partial \mathbf{p}}^{\mathrm{T}} (f(\mathbf{p}) + g(\mathbf{p})\mathbf{u}) + \frac{\partial h(\mathbf{p},t)}{\partial t} \geq -\omega(h(\mathbf{p},t))
\end{aligned} \tag{11}$$

where $\frac{\partial h(\mathbf{p},t)}{\partial t} = [\frac{\partial h}{\partial x} \ \frac{\partial h}{\partial y} \ \frac{\partial h}{\partial z}]^\top$ and $\frac{\partial h(\mathbf{p},t)}{\partial t} = \frac{\partial h}{\partial t}$ are as derived in Equation (10) and $f(\mathbf{p}) = 0, g(\mathbf{p}) = \mathbf{I}$ from the position kinematics. Moreover, for a given $(\mathbf{p},t)$, the constraint in (11) is linear in $\mathbf{u}$, with its coefficients defined by the partial derivatives in (10) and therefore, at any given time, (11) is a classical quadratic program, which can be solved efficiently at very high rates. The quadratic program can be proven to be feasible for all $\mathbf{p} \in \mathscr{X}$, such that the control input set $K_h(x)$ defined in (1) is non-empty, through Proposition 1 by following similar steps mentioned in [20].

V. Experimental Results

The performance of the proposed controller is validated on a Crazyflie 2.0 Nano Quadcopter. The Turtlebot 3 Burger, attached with a landing platform, is used as the UGV (cf. Fig. 6). The odometry for both the UGV and the UAV is obtained from a Vicon motion capture system.

The proposed landing control strategy is tested in two scenarios, as explained in the following subsections. In each scenario, the motors are turned OFF when the UAV is inside the descending cone at a relative altitude of less than 5 centimeters. The chosen control parameters are $\mathbf{K_p} = \mathbf{I}_3$, $\mathbf{K_v} = 0.5 * \mathbf{I}_3$, $\mathbf{K_1} = \text{diag}\{7,7,0.5\} * 1e4$, $\mathbf{K_2} = \text{diag}\{2.0,2.0,0.2\} * 1e4$ $v_m^x = v_m^y = 0.2\text{ms}^{-1}$, $v_m^z = 0.5\text{ms}^{-1}$, α, β are calculated to be $1.0, 1.5$ respectively by choosing $e_{zp}^* = 0.55\text{m}, \theta = 60$ deg (cf. (7)), and $w = 0.7$.

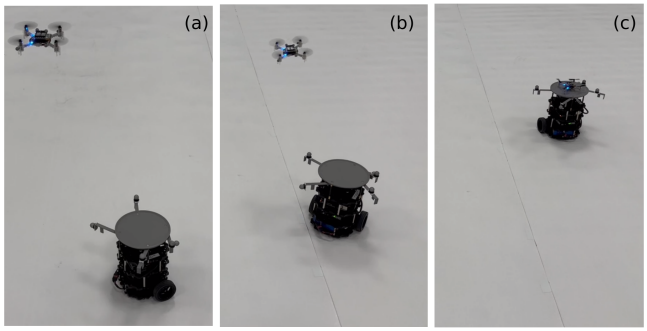

Fig. 6: UAV landing on the moving platform. (a) UAV's initial condition, (b) UAV approaches the platform, (c) UAV lands on the platform.

A. Scenario 1: Static Target

In this scenario, we evaluate the CBF's ability to shape the maneuver of the UAV to impose safety constraints while landing on a stationary platform. The relative landing trajectory of the UAV with respect to the landing spot, along with the CBF, is presented in Fig. 7. A 2-dimensional

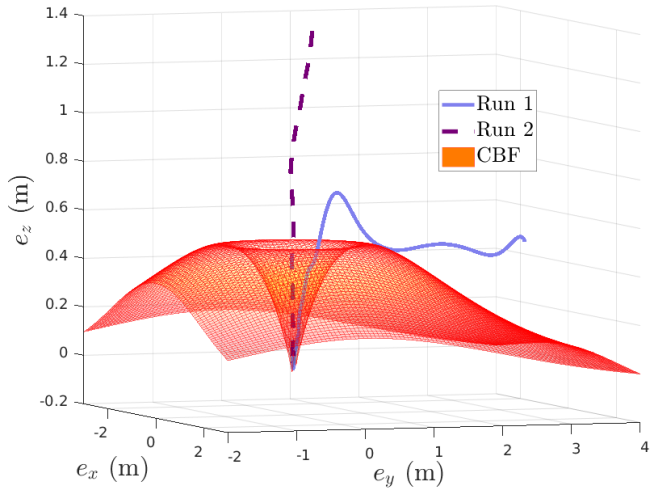

Fig. 7: Case 1: 3-dimensional representation of the CBF's boundary (red and yellow mesh) and UAV position relative to the landing spot.

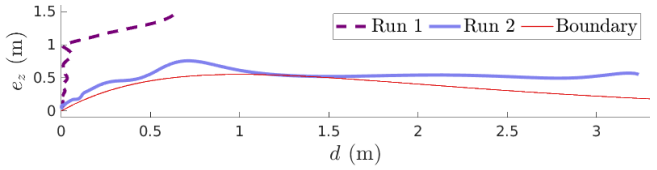

Fig. 8: Case 1: 2-dimensional representation of the relative altitude and the horizontal distance between the UAV and the UGV. The region below the red line is deemed unsafe.

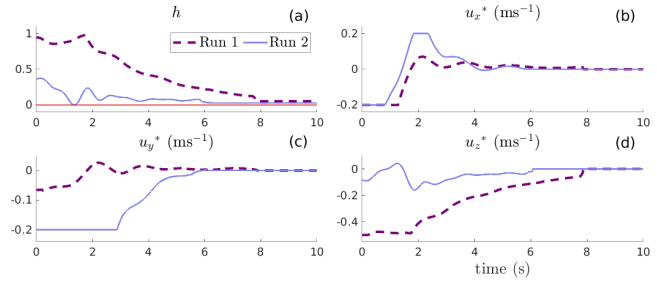

Fig. 9: Case 1; (a) Values of $h(x,y,z,t)$ over the time; (b)-(d) filtered velocity inputs along X,Y,Z directions.

projection between the relative altitude and the horizontal distance is presented in Fig 8.

In Run 1, the UAV is initiated with a larger $d(0)$ and smaller $e_z(0)$. So, the nominal control input is provided initially without the CBF filter. When the UAV approaches the CBF boundary, the CBF filter pushes the UAV above to ensure that the UAV enters the descending cone from a safe altitude. However, due to the mechanical limitations of the UAV to track the desired velocities precisely, the UAV enters the unsafe zone slightly (cf. $1-2$ seconds in Fig. 9 (a)), which further increases the filtered control input resulting in an overshoot. However, when the UAV enters the descending cone, it descends vertically towards the target. In Run 2, since the UAV is starting well above the descending cone and a smaller $d(0)$, the CBF allows the UAV to land only with the nominal control.

B. Scenario 2: Moving Target

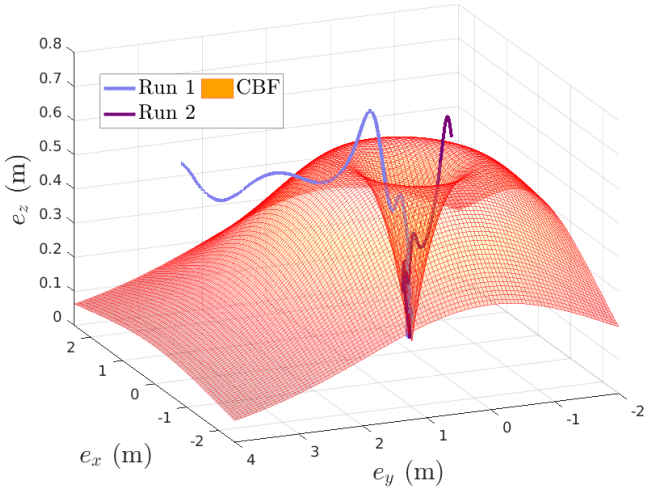

Fig. 10: Case 2: UAV's relative position with respect to the landing spot and the CBF's boundary surface (mesh). The time-varying CBF appears static in the error dimensions.

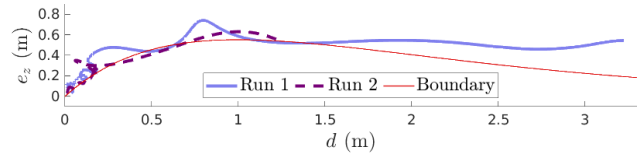

Fig. 11: Case 2: Relative altitude and the horizontal distance between the UAV and UGV.

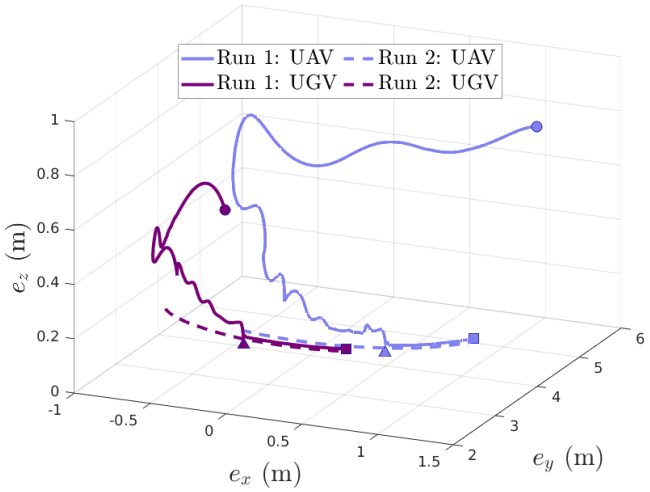

Fig. 12: Case 2: Recorded trajectories of the UAV and the UGV. Circles indicate the initial positions of the UAV, triangles indicate the points at which the UAV lands on the platform, and squares indicate the end of the trajectories.

In this scenario, we test the time-varying nature of the CBF by landing the UAV on a UGV moving with the linear

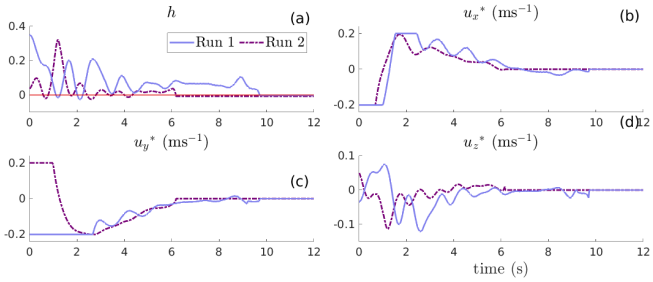

Fig. 13: Case 2: (a) Values of $h(x,y,z,t)$ over time; (b), (c), (d) Filtered velocity input in X,Y,Z axes respectively.

and angular velocities of 0.1ms^{-1}, 0.1 rad s^{-1}. In Run 1, the UAV starts from a larger $d(0)$, while the UGV moves away from the UAV. Due to this, the safe region between the UAV and UGV increases. So, the CBF filter does not act until the UAV is very close to the boundary as seen in Fig. 10. Similar to the static case, the UAV enters the unsafe zone a little (cf. at 1.2 m in Fig 11). This causes an overshoot and due to the mechanical limitations of the UAV in low-level control, the UAV enters into an oscillation when enters the descending cone (cf. the tracked UAV positions in Fig. 12). In Run 2, the UAV starts close to the descending cone but the UGV is approaching the UAV. So, though $h(0) > 0$ (cf. Fig. 13), due to the effect of $\frac{\partial h}{\partial t}$, the filter produces a positive u_z^* value (cf. Fig. 13). The UAV is pushed above the descending cone (cf. Fig. 11 at 1 m). As the UAV enters the descending cone, the UGV passes UAV horizontally resulting in a change in the direction of the error. Before the low-level controller could track the desired velocities, the UAV enters the unsafe zone slightly and the CBF pushes it back to safety causing a small oscillation (cf. Fig. 12) before landing successfully.

Remark 1 (Parameter Tuning): The experiments show that when initiated within the safe region, the filtered input forces the UAV to not leave it. Though the UAV momentarily enters the unsafe region due to the tracking limitations of the lower-lever controller, this can be fixed by decreasing the value of w. However, a lower value of w increases the overall landing duration. Further, high values of $\mathbf{K_p}, \mathbf{K_v}$ provide better tracking and faster convergence but they result in large control inputs. So, the parameters must be chosen accordingly.

VI. Conclusions

In this article, we presented a CBF-based control scheme to ensure the safe and precise landing of a UAV on a moving platform. A time-varying control barrier function (TV-CBF) was synthesized to capture the safety and precision constraints for landing. A multi-layer controller is designed involving the TV-CBF and experimentally validated in scenarios with static and moving targets. The controller landed the UAV safely in all the scenarios. As part of our future work, we are extending the proposed framework to work with modeling uncertainties and external disturbances.

References

[1] P. R. Palafox, M. Garzón, J. Valente, J. J. Roldán, and A. Barrientos, "Robust visual-aided autonomous takeoff, tracking, and landing of a small uav on a moving landing platform for life-long operation," *Applied Sciences*, vol. 9, no. 13, p. 2661, 2019.

[2] C. G. Grlj, N. Krznar, and M. Pranjić, "A decade of uav docking stations: a brief overview of mobile and fixed landing platforms," *Drones*, vol. 6, no. 1, p. 17, 2022.

[3] H. Lee, S. Jung, and D. H. Shim, "Vision-based uav landing on the moving vehicle," in *2016 International conference on unmanned aircraft systems (ICUAS)*. IEEE, 2016, pp. 1–7.

[4] Y. Meng, W. Wang, H. Han, and J. Ban, "A visual/inertial integrated landing guidance method for uav landing on the ship," *Aerospace Science and Technology*, vol. 85, pp. 474–480, 2019.

[5] Y. Zou and K. Xia, "Robust fault-tolerant control for underactuated takeoff and landing uavs," *IEEE Transactions on Aerospace and Electronic Systems*, vol. 56, no. 5, pp. 3545–3555, 2020.

[6] K. Xia, S. Lee, and H. Son, "Adaptive control for multi-rotor uavs autonomous ship landing with mission planning," *Aerospace Science and Technology*, vol. 96, p. 105549, 2020.

[7] I. Kalinov, E. Safronov, R. Agishev, M. Kurenkov, and D. Tsetserukou, "High-precision uav localization system for landing on a mobile collaborative robot based on an ir marker pattern recognition," in *2019 IEEE 89th Vehicular Technology Conference (VTC2019-Spring)*. IEEE, 2019, pp. 1–6.

[8] Y. Guo, J. Guo, C. Liu, H. Xiong, L. Chai, and D. He, "Precision landing test and simulation of the agricultural uav on apron," *Sensors*, vol. 20, no. 12, p. 3369, 2020.

[9] K. Xia, M. Shin, W. Chung, M. Kim, S. Lee, and H. Son, "Landing a quadrotor uav on a moving platform with sway motion using robust control," *Control Engineering Practice*, vol. 128, p. 105288, 2022.

[10] A. D. Ames, S. Coogan, M. Egerstedt, G. Notomista, K. Sreenath, and P. Tabuada, "Control barrier functions: Theory and applications," in *2019 18th European control conference (ECC)*. IEEE, 2019, pp. 3420–3431.

[11] W. Qing, H. Chen, X. Wang, and Y. Yin, "Collision-free trajectory generation for uav swarm formation rendezvous," in *2021 IEEE International Conference on Robotics and Biomimetics (ROBIO)*. IEEE, 2021, pp. 1861–1867.

[12] H. Dan, T. Hatanaka, J. Yamauchi, T. Shimizu, and M. Fujita, "Persistent object search and surveillance control with safety certificates for drone networks based on control barrier functions," *Frontiers in Robotics and AI*, p. 333, 2021.

[13] G. Niu, Q. Yang, Y. Gao, and M.-O. Pun, "Vision-based autonomous landing for unmanned aerial and ground vehicles cooperative systems," *IEEE robotics and automation letters*, vol. 7, no. 3, pp. 6234–6241, 2021.

[14] H. Zhou, Z. Zheng, Z. Guan, and Y. Ma, "Control barrier function based nonlinear controller for automatic carrier landing," in *2020 16th International Conference on Control, Automation, Robotics and Vision (ICARCV)*. IEEE, 2020, pp. 584–589.

[15] L. Lindemann and D. V. Dimarogonas, "Control barrier functions for signal temporal logic tasks," *IEEE Control Systems Letters*, vol. 3, no. 1, pp. 96–101, 2019.

[16] K. Alexis, G. Nikolakopoulos, and A. Tzes, "Model predictive quadrotor control: attitude, altitude and position experimental studies," *IET Control Theory & Applications*, vol. 6, no. 12, pp. 1812–1827, 2012.

[17] T. Lee, M. Leok, and N. H. McClamroch, "Geometric tracking control of a quadrotor uav on se (3)," in *49th IEEE Conference on Decision and Control (CDC)*. IEEE, 2010, pp. 5420–5425.

[18] V. N. Sankaranarayanan, S. G. Satpute, and G. Nikolakopoulos, "A survey on control design approaches for remotely operated uavs," in *2022 30th Mediterranean Conference on Control and Automation (MED)*. IEEE, 2022, pp. 389–395.

[19] S. Ganguly, V. N. Sankaranarayanan, B. Suraj, R. D. Yadav, and S. Roy, "Robust manoeuvring of quadrotor under full state constraints," *IFAC-PapersOnLine*, vol. 55, no. 1, pp. 32–37, 2022.

[20] A. Saradagi, A. Banerjee, S. Satpute, and G. Nikolakopoulos, "Safe autonomous docking maneuvers for a floating platform based on input sharing control barrier functions," https://arxiv.org/abs/2209.06618, 2022. [Online]. Available: https://arxiv.org/abs/2209.06618